Journal of Applied Sciences

ISSN 1812-5654

science alert

ANSInet
an open access publisher
http://ansinet.com

Journal of Applied Sciences 11 (2): 367-372, 2011
ISSN 1812-5654 / DOI: 10.3923/jas.2011.367.372

The Effect of Tool Surface Roughness in Cold Work Extrusion

S. Syahrullail, C.S.N. Azwadi, M.R. Abdul Kadir and N.E.A. Shafie
Faculty of Mechanical Engineering, Universiti Teknologi Malaysia, 81310 UTM Skudai, Johor, Malaysia

Abstract: In this study, the influence of tool surface roughness on the metal flow in deformation areas was investigated by using a cold work plane strain extrusion apparatus. Two types of polished tools (taper die) were used in this experiment. The tool (taper die) had a 45-degree die half angle. The material of specimen (billet) was pure Aluminum A1100. The lubricant used in this investigation was Refined, Bleached and Deodorized (RBD) palm olein. The extrusion process was done by using a hydraulic press machine. The extrusion load and piston stroke movement were recorded by using the load cell and displacement sensor, respectively. After the experiment, the billet was taken out and the surface roughness was measured. The u- and v- component velocities were calculated using the visioplasticity method. As a result, the extrusion load and surface roughness of extruded material differed between the two types of taper die and influenced the metal flow in the deformation area of billets.

Key words: Extrusion, palm olein, taper die, surface roughness, visioplasticity

INTRODUCTION

Surface roughness is an important parameter of evaluation in mechanical engineering. In fluid mechanics, the high surface roughness of an object would increase the drag coefficient of that object, especially for streamlined bodies. A small amount of surface roughness can greatly affect the properties of the turbulent boundary layer, such as momentum thickness and local skin friction. For blunt bodies, such as a circular cylinder and sphere, the drag coefficient decreases when the surface roughness increases (Cengel and Cimbala, 2006).

In metal forming, the surface roughness of tools would influence the lubrication condition between the tool and the formed material's surface. At the same time, different surface roughness would give different friction conditions. This phenomenon plays an important role in producing a product with a glossy surface finish. For example, forging experiments have shown that when low viscosity lubricants are used, there is a clear delineation of the grain boundaries and the appearance of slip lines in the product surface (Jung *et al*., 2008). The surface roughness of a tool in metal forming is not specified very well. In general, it is either approximately one quarter of the lubricant film thickness or the natural roughness found at similar strains in free surface deformation, whichever is smaller (Schey, 1984).

The mechanisms that control the surface roughness of the product is thin lubricant films (tooling control) the strip conformed to the roll so that their roughness became familiar (Schey, 1984). The lubrication analysis showed that the oil film thickness must be smaller than the surface roughness to achieve an appropriate surface finish (Pilarczyk *et al*., 1998). Therefore, lubricants prevent direct metallic contact, with the reduction of extrusion loads, friction and wear improves the product's quality and the tool's life.

Vegetable oils have the potential to be used as a metal forming lubricant. It has an advantage in reducing the forming load. The existence of fatty acids in vegetable oil could help the lubricant to stick very well to the tool's surface. It would create a boundary lubrication condition and could produce a product with low surface roughness. In Malaysia, palm oil has the potential to be used as the base oil in producing bio-lubricant. Palm oil is environmentally friendly and has a high biodegradability rate compared to petroleum based mineral oil. Palm oil also has a high production rate, which is an average 3.74 tons of oil per hectare every year (Ming and Chandramohan, 2002).

In this study, the influence of a tool's surface roughness on the extruded product is studied by using a cold work plane strain extrusion apparatus. The test lubricant was RBD palm olein and the test material was pure aluminum A1100. Analysis were focused on extrusion load, surface finishing and velocity in the deformation area. Results showed that the roughness of the taper die influences the metal flow and the product surface conditions.

Corresponding Author: S. Syahrullail, Faculty of Mechanical Engineering, Universiti Teknologi Malaysia, 81310 UTM Skudai, Johor, Malaysia

MATERIALS AND METHODS

This study was conducted at Fluid Laboratory, Faculty of Mechanical, Universiti Teknologi Malaysia, Skudai, Johor. The duration of the project is July 2009 to December 2009.

Experimental apparatus: A schematic sketch of the cold work plane strain extrusion apparatus is shown in Fig. 1a and b. The main components of this apparatus are the container wall, taper die and workpiece (called the billet).

The taper die, which is shown in Fig. 2a and b, is made from tool steel SKD11 and the necessary heat treatments were done before the experiments. The taper die has a 45-degree die half angle and a 5 mm die bearing. The surface of the taper die that contacts the billet is called the experimental surface of taper die. Two types of taper dies were constructed: taper die 3 P and 1 P. Taper die 3 P has three areas that were polished with an abrasive paper and has a surface roughness (Ra) of approximately 0.05 micron. Taper die 1 P has one area that was polished with an abrasive paper and has a surface roughness (Ra) of approximately 0.05 micron. The other two areas were polished slightly and have a surface roughness (Ra) of approximately 1.0 micron. For all experimental conditions, a specified amount of lubricant was applied to these surfaces before the experiments. The same type of lubricant was applied to the other surfaces of the experimental apparatus. Both types of taper die had a Vickers hardness of 650 Hv.

Figure 3 shows a schematic sketch of the billets that were used in the experiments. The billet material was pure aluminum A1100. The billet shape was produced using an NC wire cut electric discharge machining device. Two similar billets were stacked and used as a single unit of billet. One side of the contact surface of the combined

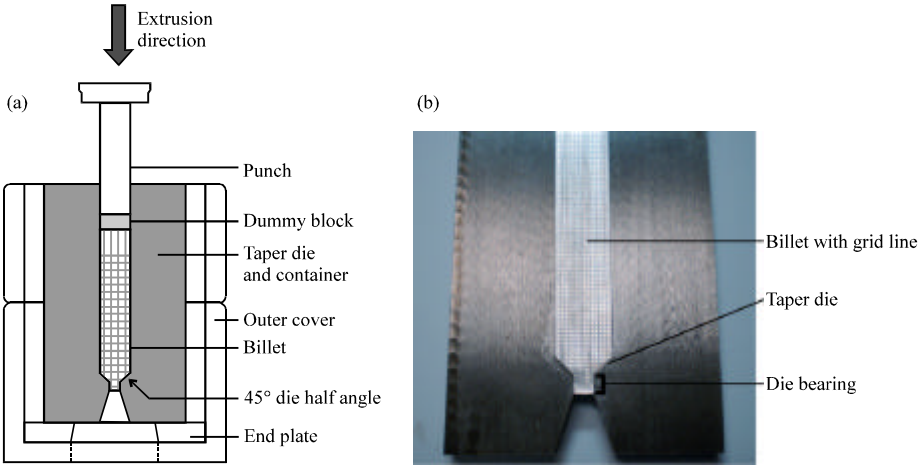

Fig. 1: (a) A schematic sketch of plane strain extrusion apparatus and (b) a photograph of the taper die and billet

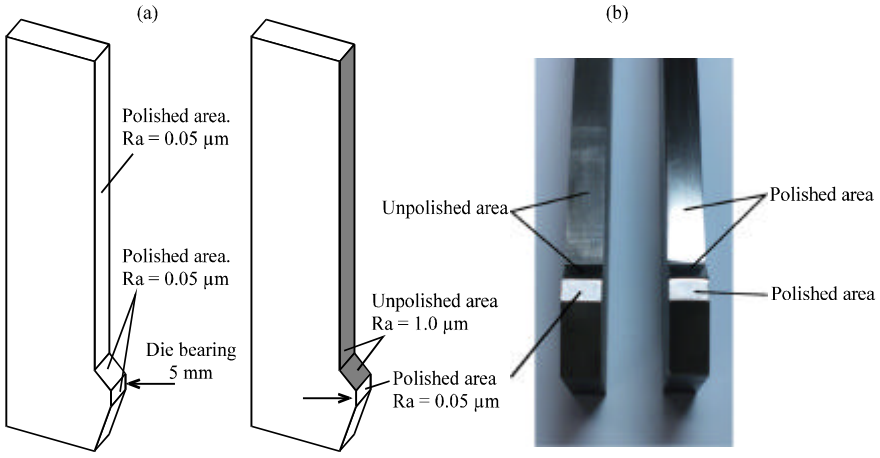

Fig. 2: (a) A schematic sketch of taper die with three polished area (3 P) and one polished area (1 P) and (b) a photograph of the 3 P and 1 P taper die

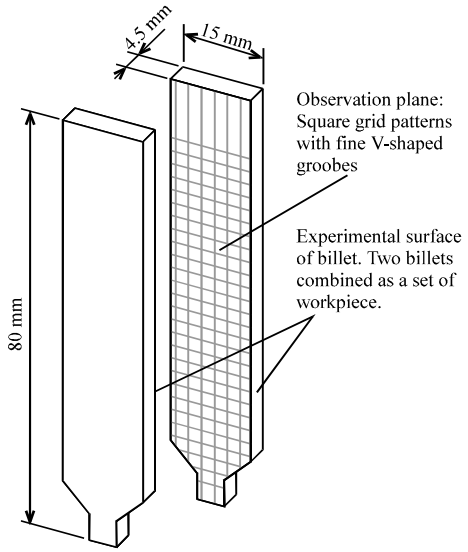

Fig. 3: A schematic sketch of combination of billets used in the experiments

Table 1: Properties of RBD palm olein

Properties	Value
FFA (m.w. 256, palmitic)	Max 0.1%
Slip melting point	Max 24°C
IV	Min 56
Color 5¼ lovibond	Max 3 red (optional 6 R)
Kinematic viscosity at 30°C (mm^2 sec^{-1})	34

billets was the plastic flow observation plane during plane extrusion. The observation plane was not affected by the frictional constraint of the parallel side walls. A square grid pattern to measure the material flow during the extrusion process was scribed by the NC milling machine onto the observation plane of the billet. The grid lines were V-shaped grooves that were 0.5 mm deep, 0.2 mm wide and 1.0 mm in interval length. The billets were annealed before the experiments. The experimental surface of the billet (the surface that contacts the taper die) had a surface roughness of approximately 2.5 micron and its Vickers hardness was 30 Hv.

Test lubricant: The test lubricant was RBD palm olein, written as PO. The RBD is an abbreviation for refined, bleached and deodorized. Palm olein is the liquid fraction that is obtained by the fractionation of palm oil after crystallization at a controlled temperature. In these experiments, a standard grade of RBD palm olein, which was incorporated in the Malaysian Standard MS 816:1991, was used. The properties of RBD palm olein is shown in Table 1. The test lubricant was applied onto the experimental surface of the taper die before the experiment. The amount of lubricant used was 5 mg (0.52 mg cm^{-2}). The mass measurement was done with a digital balance that had a tolerance of 0.1 mg.

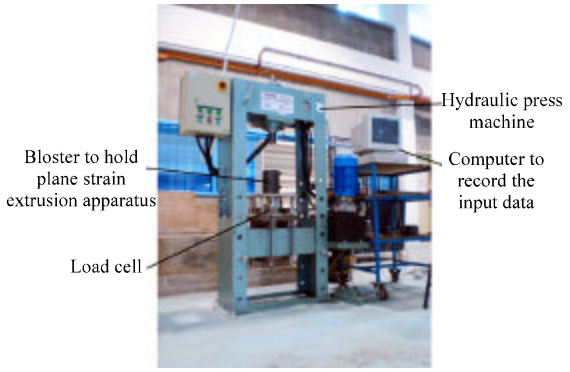

Fig. 4: The hydraulic press machine, load cell location and the data acquisition system

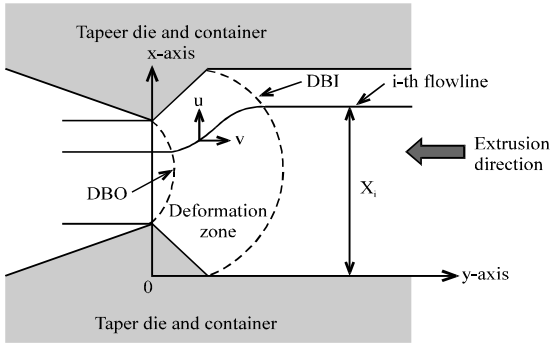

Fig. 5: Axis system used in the visioplasticity method

Experimental procedure: Lubricant was applied onto the taper die and the billets were cleaned with acetone. Then the taper die and billets were assembled as shown previously in Fig. 1. The plane strain extrusion apparatus was assembled and placed onto the hydraulic press machine as shown in Fig. 4. The load cell and displacement sensor were used to record the extrusion load and ram displacement; the data was saved in a computer. The experiments were carried out at room temperature. The extrusion was stopped at a piston stroke of about 35 mm where the extrusion process was in a steady state condition. The ram speed was about 9.4 to 9.8 mm sec^{-1}. After the experiment, the partially extruded billets were removed from the plane strain extrusion apparatus and the combined billets were separated for the grid line tracing, surface roughness measurement and visioplasticity analysis. The explanation for billet grid line (flowline) tracing was discussed in a previous publication; the details are omitted here (Syahrullail *et al*., 2009). The billet grid lines were traced and the digital data of the flowlines based on the axis shown in Fig. 5 were plotted. The visioplasticity calculation started with the calculation of flow function, followed by the velocities components, the strain rate components, the effective strain rate and the effective

strain. Since, the details of the analytical calculation procedure was explained in an earlier publication, it is omitted here (Syahrullail *et al*., 2005).

Flow function:

$$\psi_i = X_i|V_o| \quad (1)$$

Velocity component (Velocity in x-direction: u, velocity in y-direction: v).

$$u = \frac{\partial \psi}{\partial Y}, \quad v = \frac{\partial \psi}{\partial X} \quad (2)$$

The strain rate component (s-1).

$$\dot{\varepsilon}_X = \frac{\partial u}{\partial X}, \quad \dot{\varepsilon}_Y = \frac{\partial v}{\partial Y}, \quad \dot{\gamma}_{XY} = \frac{\partial u}{\partial Y} + \frac{\partial v}{\partial X} \quad (3)$$

The effective strain rate (s-1):

$$\dot{\varepsilon} = \frac{2}{3}\sqrt{3\dot{\varepsilon}_X^2 + \frac{3}{4}\dot{\gamma}_{XY}^2} \quad (4)$$

The effective strain (time integration value of the effective strain rate along the flow line):

$$\varepsilon = \int \dot{\varepsilon}\, dt \quad (5)$$

In the equations, V_o is the velocity of the press ram in mm sec^{-1} and Xi is the distance in mm from the y-coordinate axis (X = 0) of the i-th flow line in the region where deformation does not occur. In this study, the plastic flow velocities in the deformation zone were calculated and mutually compared. The effective strain for both experimental conditions were shown no obvious change.

RESULTS

Extrusion load: Throughout the extrusion process, all data of extrusion load and piston stroke were detect by the load cell and displacement sensor. After the experiment, the extrusion load-piston strike curves were plotted and shown in Fig. 6. The Fig. 6 shows that the extrusion load reached a constant level during the process and that the extrusion process became a steady state condition at a piston stroke of more than 25 mm. The extrusion load value at piston stroke 35 mm for taper die 3 P and 1 P are 57 kN and 48 kN, respectively.

Surface roughness: The values of the arithmetic mean surface roughness (Ra) along the experimental surface of the billet were measured with a surface profiler device. The measure direction was perpendicular to the extrusion

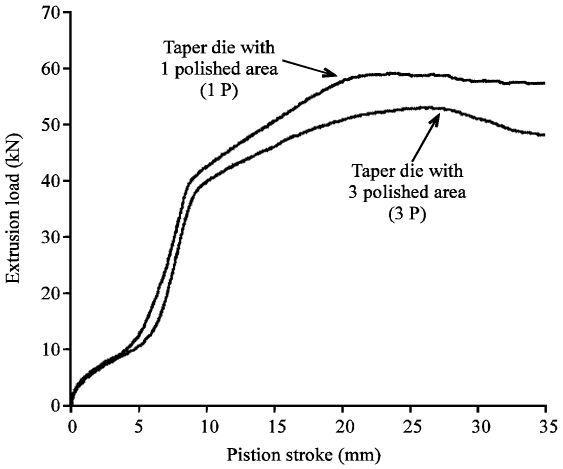

Fig. 6: Extrusion load-piston stroke curves

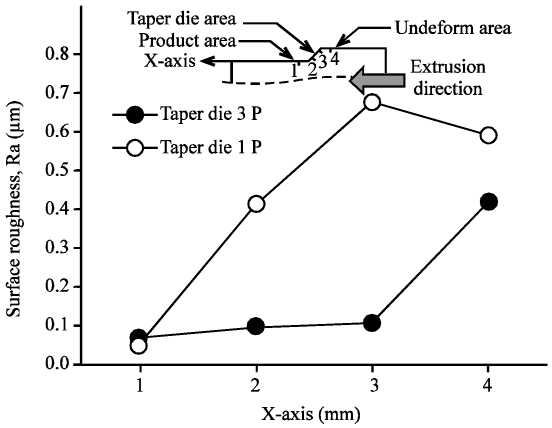

Fig. 7: Surface roughness distribution on the experimental surface of billet

direction. The experimental surface of the billet was the surface of the billet that contacts the taper die and the container wall. The experimental surface of the billet was labeled as the X-axis. Four major points were measured. Point 1 was located at product area of the billet, where the extrusion process was finished. Point 2 was located at the taper die near the exit, where the deformation of the billet was almost finished. Point 3 was located at taper die near the inlet, where the deformation of billet was just begun. Point 4 was located at the area where the billet was not deformed (the billet was still in its original size). The distribution of surface roughness is shown in Fig. 7.

Relative sliding velocity: From the tracing data, the velocity component of the billet that slides on the taper die's surface was calculated using the visioplasticity method. Then, the velocities component values were divided with ram speed V_o to get the relative

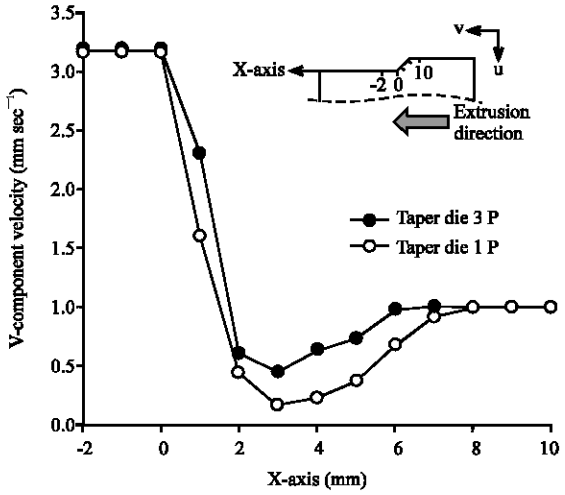

Fig. 8: v-component velocity distribution along the experimental surface of billet

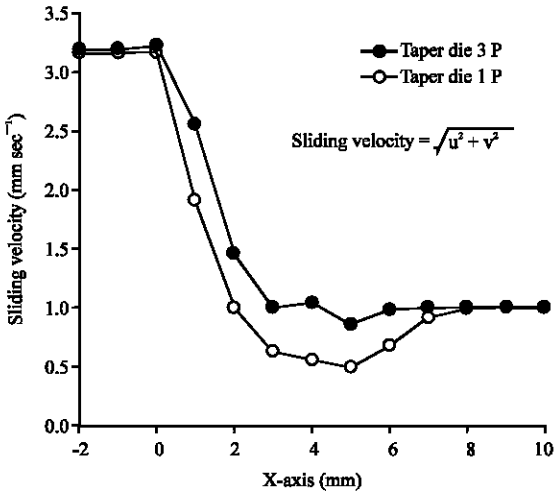

Fig. 10: Sliding velocity of the extruded billet

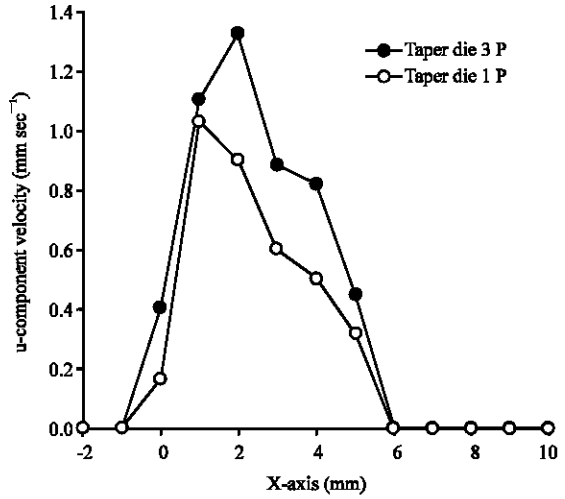

Fig. 9: u-component velocity distribution along the experimental surface of billet

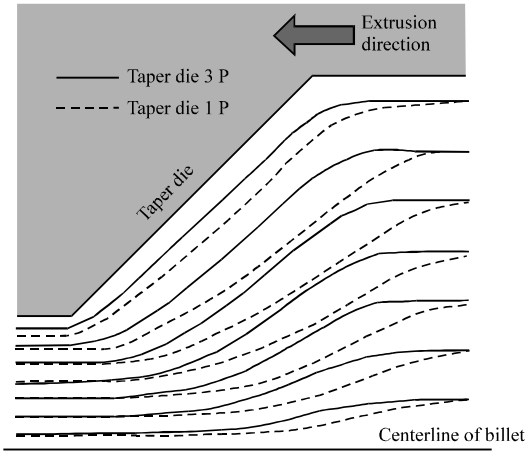

Fig. 11: Mutual comparison of metal flow in the deformation area of billet

component velocity. Comparisons of the relative velocity of the v- (horizontal direction velocity) and u- (vertical direction velocity) of the plastic flow velocity along the experimental surface of the billet are shown in Fig. 8 and 9, respectively. The resultant relative sliding velocity distribution is shown in Fig. 10. The resultant relative sliding velocity was calculated using Eq. 6, where u represents the relative u-component velocity and v represents the relative v-component velocity.

$$\text{Resultant sliding velocity} = \sqrt{u^2 + v^2} \quad (6)$$

Flowline observation: To understand the behavior of the billet's metal flow extruded in this experiment, the horizontal flowlines were compared mutually. Since, the billet has a symmetrical shape, the horizontal flowlines were compared for only half part of the billet. Figure 11 shows a mutual comparison of the horizontal flowlines for billet extruded with taper die 3 P and 1 P.

DISCUSSION

The extrusion load for the experiment using the taper die 1 P is higher than the extrusion load for taper die 3 P (Fig. 6). The extrusion load difference at a piston stroke of 35 mm is about 9 kN. The rough surface at the taper die and container wall area gave more metal-to-metal contact and it increased the frictional constraint between the tool and billet. At the same time, it increased the extrusion load (Monaghan and O'Reilly, 1996).

The surface roughness (Fig. 7) of the extruded product (at point 1) for both taper die 3 P and 1 P was

almost similar. The average value of surface roughness for point 1 for both taper die types ranged from 0.07 to 0.09 micron. An observation of the product area surface, through the use of a CCD camera, found no severe wear.

The surface roughness for the billet (at points 2 and 3) that was extruded with taper die 1 P has a higher value compared to those extruded with taper die 3 P. For both taper die, due to the no severe wear was occurred, we found that the lubrication condition at point 2 and 3 is mixed lubrication condition. For taper die 1 P, the thickness of the lubricant between the taper die surface and the billet was very thin so the billet reflected the taper die condition very well (Wilson and Weiming, 2001). It is caused the billet surface that contact the taper surface reflect the coarse surface of the taper die. However, for taper die 3 P, the billet has a smooth surface because of the smooth surface of the taper die. The rough tool surface would give high frictional constraint and then the extrusion load for billet extruded with taper die 1 P was higher compared to taper die 3 P. This result shows that tool surface roughness would influence the lubricant film thickness between the billet and taper die surface. However, the effect of tool surface roughness on the product area was not as obvious.

The rougher the tool's surface, the higher the possibility to create high friction between the tool (taper die) and billet due to the increment of metal-to-metal contact. Taper die 3 P, which had three polished areas, showed the increment of the velocity compared to those extruded with taper die 1 P (Fig. 8-10), showing that the taper die 3 P gave less frictional constraint compared to taper die 1 P. This result was similar compared to the analytical results made by Pan and Sansome (1982) and Betancourt-Dougherty and Smith (1998).

From Fig. 11, the taper die 1 P created a high friction between the tool and the billet surface causing the metal to flow to the inner side of the billet. For the billet that was extruded with taper die 3 P, the smooth tool surface resulted in a low friction condition that caused the metal to flow near the taper die area. This result has a good agreement with the results published by Wu and Hsu (2002).

CONCLUSIONS

The influences of the tool surface roughness on the plasticity flow were investigated with a cold work plane strain extrusion apparatus. The results show that a tool (taper die) with a rough surface has the possibility to create high friction conditions due to its increment in metal-to-metal contact area. This would increase the extrusion load and affect the metal flow of the extruded material during the extrusion process. However, there is no obvious different at product surface quality.

ACKNOWLEDGMENTS

The authors would like to thanks to the Mechanical Engineering Faculty at the Universiti Teknologi Malaysia for their cooperation during the preparation of this study. The authors also wish to thank the Ministry of Higher Education, Malaysia for financial support through the grant vote 78604.

REFERENCES

Betancourt-Dougherty, I.C. and R.W. Smith, 1998. Effects of load and sliding speed on the wear behaviour of plasma sprayed TiC-NiCrSi coatings. Wear, 217: 147-154.

Cengel, Y.A. and J.M. Cimbala, 2006. Fluid Mechanics Fundamentals and Application. McGraw-Hill International, New York, ISBN: 007-124934-6.

Jung, K.H., H.C. Lee, S.H. Kang and Y.T. Im, 2008. Effect of surface roughness on friction in cold forging. J. Achieve. Mat. Manuf. Eng., 31: 327-334.

Ming, K.K. and D. Chandramohan, 2002. Malaysian palm oil industry at crossroad and its future direction. Oil Palm Ind. Econ. J., 2: 10-15.

Monaghan, J. and M. O'Reilly, 1996. The influence of lubrication on the surface finish of cold forged components. J. Materials Process. Technol., 56: 678-690.

Pan, D. and D.H. Sansome, 1982. An experimental study of the effect of roll-speed mismatch on the rolling load during the cold rolling of thin strip. J. Mechanical Working Technol., 6: 361-377.

Pilarczyk, J.W., H. Dyja, B. Golis and E. Tabuda, 1998. Effect of roller die drawing on structure, texture and other properties of high carbon steel wires. Metals Mater., 4: 727-731.

Schey, J.A., 1984. Tribology in Metalworking-Friction, Lubrication and Wear. American Society for Metals, USA., ISBN: 0-87170-155-3.

Syahrullail, S., C.S.N. Azwadi and W.B. Seah, 2009. Plasticity analysis of pure aluminium extruded with anrbd palm olein lubricant. J. Applied Sci., 9: 3581-3586.

Syahrullail, S., K. Nakanishi and S. Kamitani, 2005. Investigation of the effects of frictional constraint with application of palm olein oil lubricant and paraffin mineral oil lubricant on plastic deformation by plane strain extrusion. J. Jap. Soc. Tribologist, 50: 877-885.

Wilson, W.R.D. and L. Weiming, 2001. Mechanics of surface roughening in metal forming processes. J. Manuf. Sci. Eng., 123: 279-283.

Wu, C.Y. and Y.C. Hsu, 2002. The influence of die shape on the flow deformation of extrusion forging. J. Mater. Process. Technol., 124: 67-76.